

**Exercise injects for a Hikurangi Subduction Zone
earthquake aftershock sequence**

DR Burbidge
WL Power

DA Rhoades
S-L Lin

A Christophersen
JS Becker

**GNS Science Consultancy Report 2019/130
August 2019**



DISCLAIMER

This report has been prepared by the Institute of Geological and Nuclear Sciences Limited (GNS Science) exclusively for and under contract to East Coast Life at the Boundary (East Coast LAB). Unless otherwise agreed in writing by GNS Science, GNS Science accepts no responsibility for any use of or reliance on any contents of this report by any person other than East Coast LAB and shall not be liable to any person other than East Coast LAB, on any ground, for any loss, damage or expense arising from such use or reliance.

Use of Data:

Date that GNS Science can use associated data: 1 September 2019

BIBLIOGRAPHIC REFERENCE

Burbidge DR, Rhoades DA, Christophersen A, Power WL, Lin S-L, Becker JS. 2019. Exercise injects for a Hikurangi Subduction Zone earthquake aftershock sequence. Lower Hutt (NZ): GNS Science. 16 p. Consultancy Report 2019/130.

CONTENTS

EXECUTIVE SUMMARY	III
1.0 INTRODUCTION	1
2.0 SUMMARY OF THE HISTORY OF TSUNAMIGENIC AFTERSHOCKS	2
2.1 Tohoku 2011 Aftershock Sequence	2
2.2 Sumatra 2004 Sequence	3
2.3 New Ireland 2000 Sequence.....	3
2.4 Alaska 1964 Sequence.....	3
2.5 Chile 1960 Sequence	3
2.6 Summary	4
3.0 HYPOTHETICAL EARTHQUAKE CATALOGUE AND VIDEO	5
4.0 FORECAST PROBABILITY OF A MMI VI OR GREATER EARTHQUAKE	6
5.0 MMI FROM THE LARGEST AFTERSHOCK	8
6.0 PROBABILITY OF A TSUNAMIGENIC AFTERSHOCK	11
7.0 QUALITATIVE AFTERSHOCK IMPACT ASSESSMENT	12
7.1 Big Picture	12
7.2 Wellington, Porirua and Hutt Valley	12
7.3 Greater Wellington Region.....	14
7.4 Outside Greater Wellington Region	14
7.5 Aftershock Sequence.....	14
8.0 ACKNOWLEDGEMENTS	15
9.0 REFERENCES	15

FIGURES

Figure 3.1	The proposed earthquake aftershock sequence for the scenario.....	5
Figure 4.1	The probability that a point experiences shaking at above MMI VI from an aftershock generated by the M8.9 mainshock over the following 12 months.	7
Figure 5.1	Estimated MMI ground motion intensities for the mainshock rupture calculated using Shakemap.	9
Figure 5.2	Estimated MMI ground motion intensities for the largest aftershock in the sequence calculated using Shakemap.....	10
Figure 6.1	The average probability (%) of one or more Mw 7 or larger to follow a mainshock of magnitude 8.9 within the next year (red), month (blue) and day (black) for a year after the mainshock.	11

ADDITIONAL FILES

A map of the proposed foreshock and aftershock sequence.....	Dropbox folder
The forecast probability of Modified Mercalli Intensity (MMI) shaking of VI or greater in the following year for the sequence.....	Dropbox folder
A map showing the MMI from the largest aftershock in that sequence.....	Dropbox folder
A figure showing the approximate probability of a potentially tsunamigenic aftershock as function of time.....	Dropbox folder
An animation of the first day of the sequence.....	Dropbox folder

EXECUTIVE SUMMARY

East Coast Life at the Boundary (East Coast LAB) have contracted GNS Science (GNS) to provide a series of exercise injects for the Hikurangi Response Plan earthquake scenario previously developed for the Hawkes Bay Civil Defence and Emergency Management (CDEM) Group. GNS previously provided Hawkes Bay CDEM with a range of injects for the possible effects and impacts of a magnitude 8.9 earthquake along the Hikurangi Subduction Zone. This report provides East Coast LAB with some additional information about the possible aftershocks generated by this scenario earthquake to be used as further injects for the exercise. Specifically, it provides the following:

1. A brief summary of any historical aftershocks that caused, or may have caused, tsunamis.
2. A map of an aftershock sequence from a historical event of similar size to the scenario relocated and reoriented to be off the east coast of the North Island instead of its historical location.
3. A map showing the forecasted probability of a Modified Mercalli Intensity (MMI) shaking of VI or greater in the following year for that sequence.
4. A map showing the MMI from the largest aftershock in that sequence.
5. A graph estimating the approximate probability of a potentially tsunamigenic aftershock as a function of time.
6. A qualitative assessment of the potential impact of an aftershock and/or tsunami.

A very simple animation of the aftershock sequence suitable for use as an exercise inject and in any associated workshops with emergency planners also accompanies the report.

In this report we base the proposed aftershock sequence on that which followed the Tohoku earthquake in 2011. We also look specifically at the potential impacts of the largest aftershock in this hypothetical sequence, a magnitude 7.7 earthquake underneath the Wellington region that occurs half an hour after the mainshock. Not surprisingly, the effects of the aftershock of this size and location would significantly further worsen the impact of the earlier magnitude 8.9 mainshock in the Wellington region.

Given that the aftershock occurs mostly onshore and only just after the mainshock, it would not make the tsunami from the mainshock significantly worse. The mainshock's tsunami would only have just started to arrive in Wellington at the time of the aftershock and would be significantly larger than any tsunami produced by this aftershock. This would be consistent with many of the historic aftershocks described in the report which often occur in the first few hours after the mainshock and do not produce a clear tsunami of their own. However, in the weeks, months or years after the aftershock there would be a significant increase in both the shaking and tsunami hazard faced by the east coast of the North Island from the extended aftershock sequence produced by a mainshock of this size. Over the first year after the mainshock the east coast of the North Island has close to 100% probability of experiencing shaking above Modified Mercalli VI from an aftershock. Even a year after the mainshock there is still a significant (about 50%) probability of an offshore magnitude 7 or greater earthquake over the following year.

This page left intentionally blank.

1.0 INTRODUCTION

East Coast Life at the Boundary (East Coast LAB) have contracted GNS Science (GNS) to provide a series of exercise injects for the Hikurangi Response Plan earthquake scenario previously developed by GNS for Hawkes Bay Civil Defence and Emergency Management (CDEM) Group. The Hawkes Bay CDEM Group are currently developing a response plan for a major Hikurangi earthquake and tsunami as part of a CDEM Resilience Fund project entitled “Hikurangi Response Plan – developing a coordinated response to a subduction rupture to assist and enhance community resilience across the North Island East Coast”. As part of the process of developing the plan, a workshop was held in June 2018 to discuss possible options for a scenario for the response plan. At the workshop the participants decided to base the scenario around a magnitude 8.9 (moment magnitude, referred to as Mw from here on) earthquake on the Hikurangi subduction zone. Following the workshop GNS developed a range of possible scenarios and provided figures and animations of the tsunami and ground shaking such an event might cause (provided under GNS project # 410W1471).

East Coast LAB have requested additional information about the scenario to provide as injects into an exercise. Specifically, they requested the following pieces of information to be provided:

1. A brief summary of any historical aftershocks that caused, or may have caused, tsunami.
2. A map of the aftershock sequence from a historical event of similar size to the scenario relocated and reoriented to be off the east coast of the North Island instead of its historical location.
3. A map showing the forecasted probability of a Modified Mercalli Intensity (MMI) of VI or greater in the following year for that sequence.
4. A map showing the MMI from the largest aftershock in that sequence.
5. A graph estimating the approximate probability of a potentially tsunamigenic aftershock as function of time (after a date following the earthquake to be determined in consultation with East Coast LAB).
6. A qualitative assessment of the potential impact of an aftershock and/or tsunami.
7. A very simple animation of the aftershock sequence suitable for use as an exercise inject and in any associated workshops with emergency planners.
8. A short letter report describing briefly how GNS put the above maps and datasets together and the other information described above.

This report is the final deliverable mentioned above. In the next sections we will summarise the work done to provide each of these injects. The maps, animation and figures themselves accompany this report.

2.0 SUMMARY OF THE HISTORY OF TSUNAMIGENIC AFTERSHOCKS

It is rare for any of the aftershocks immediately following a major offshore earthquake to clearly produce a tsunami of their own. This is because the tsunami produced by the mainshock typically continues for many hours to days following the mainshock. Any tsunami produced by an aftershock during this period is usually much smaller than the tsunami produced by the initial mainshock. It is therefore often difficult to clearly extract the tsunami signal caused by an aftershock from that caused by the mainshock if the aftershock occurs during this time.

The other potential complexity is the definition of an aftershock itself. The most common definition of an aftershock is that it is any earthquake that follows a mainshock in the following days, months or years which lies within about a single rupture length of the mainshock and is at least 1 magnitude unit smaller than the mainshock (see e.g. Scholz 2002). However, statistically a foreshock can be viewed as a mainshock that happened to have a larger aftershock and there is no distinction in magnitude (Christophersen and Smith 2008). Also, aftershock activity can continue for a very long time: in case of the Nobi, Japan earthquake for more than 100 years (Utsu et al. 1995). Thus, whether a particular earthquake is an aftershock or not is sometimes disputed. Particularly if it does not occur immediately after the mainshock (i.e. within the next few days or weeks). In those cases, some may argue that a particular earthquake may have been independent of the mainshock and simply occurred in the same general area by chance.

However, despite these complexities, definite aftershocks of great (Mw 8.0+) earthquakes are very large and would seem large enough to potentially generate their own tsunami. Aftershocks of the largest earthquakes (above Mw 9.0) are often large earthquakes themselves and can sometime have magnitudes in the high 7s or more. Earthquakes of this size would normally be expected to generate a tsunami of some sort if they were shallow, offshore and had the appropriate earthquake mechanism.

In the next few sections, we briefly go through some of the major earthquakes of the last sixty years to see if there is any evidence that any of them produced tsunamigenic aftershocks. It is mostly based on a review of the relevant earthquake and tsunami databases and the recent scientific literature.

2.1 Tohoku 2011 Aftershock Sequence

The magnitude Mw 9.1 (Mw stands for moment magnitude) Tohoku, Japan earthquake on 11 March 2011 was followed by three earthquakes above 7.0 in the first few hours after the earthquake (Mw 7.1, 7.6 and 7.9, source: GEM-ISC catalogue). Given they occurred so close to the mainshock it is not known if they were themselves tsunamigenic. In the months following the Tohoku earthquake there was a Mw 7.1 earthquake on 7 April 2011 and a 7.0 on 10 July 2011. Both of these caused measurable, but not hazardous, tsunami (8 cm and 9 cm maximum recorded amplitude respectively. Source: National Geophysical Data Centre/World Data Service's Global Historical Tsunami Database, referred to as GHTD from now on). The area offshore Honshu also experienced two other earthquakes above Mw 7 in the following few years, but whether they are aftershocks depends somewhat on the definition. According to GHTD, the Mw 7.2 that occurred on 7 December 2012 had a maximum recorded run-up height of 1.0 m and the Mw 7.1 on 25 October 2013 had a maximum recorded run-up of 0.4 m. There are no reports of damage from any of these tsunami in GHTD.

2.2 Sumatra 2004 Sequence

On 26 December 2004 Sumatra, Indonesia experienced a Mw 9.1 earthquake and Indian Ocean wide tsunami. The tsunami is estimated to have caused approximately 230,000 deaths (source: GHTD). The next tsunami in the area came from the Mw 8.6 earthquake on the 28 March 2005 (often called the Nias earthquake). It occurred to the east of the 2004 earthquake further along the Sunda Arc Subduction Zone. This earthquake also caused a significant tsunami, albeit much smaller than the one the previous year. According to GHTD, the maximum water (run-up) height of the tsunami from the Nias earthquake was 4.2 m and it caused 10 deaths. About 1200 people may have been killed by the earthquake itself. However, the Mw 8.6 earthquake is argued by some to be an independent of the 2004 earthquake, rather than an aftershock (e.g. Galahaut and Galahaut 2005). There are no records in GHTD of any other tsunami from the aftershocks of the 2004 earthquake.

2.3 New Ireland 2000 Sequence

On November 2000 a Mw 8.0 strike-slip earthquake occurred offshore New Ireland, Papua New Guinea. The earthquake was followed by a series of aftershocks with a thrust mechanism, including two above Mw 7.0. One of these two aftershocks occurred three hours after the mainshock and the other the following day. The earthquake sequence generated locally damaging tsunami on the islands of New Ireland and nearby New Britain, Bougainville and Buka (Geist and Parsons 2005). Strike-slip earthquakes normally cause the sea floor to move mostly horizontally and as a result they do not normally cause very large tsunamis. Geist and Parsons (2005) numerically modelled the tsunami from the mainshock and the two largest aftershocks and argued that the largest component of the tsunami was probably caused by one of the aftershocks rather than by the mainshock itself. However, all three probably generated tsunami of some sort. Earthquakes with a thrust mechanism (like the two largest aftershocks) cause larger amounts of vertical motion of the sea floor than strike-slip ones and are thus generally more effective at causing a tsunami, so this theory is plausible.

2.4 Alaska 1964 Sequence

On 28 March 1964, the largest earthquake in North America occurred off the coast of Alaska. Its magnitude is generally taken to be about Mw 9.2. The earthquake caused a Pacific-wide tsunami, approximately 124 deaths and \$116M damage. This earthquake also produced numerous aftershocks but they were all below Mw 6.5 according to the International Seismological Centre's Global Earthquake Model Catalogue (ISC-GEM) catalogue. GHTD does not record any tsunami coming from any of these earthquakes.

2.5 Chile 1960 Sequence

On 22 May 1960 the largest earthquake in recorded history occurred offshore Chile. The magnitude of the earthquake is typically estimated to be about Mw 9.5. It caused a major tsunami that affected many locations across the Pacific and killed about 2000 people (source GHTD). This earthquake generated numerous aftershocks, include two Mw 7.0 earthquakes on 20 June 1960, neither of which caused a clearly observable tsunami according to GHTD. However, a tsunami warning was issued on 24 May 1960 following some low mid-magnitude 6 aftershocks due to oscillations seen in South American tide gauge data. No indications of a tsunami were seen in Hawaiian gauges records following the warning. GHTD suggest the observations in South America were mostly likely from the mainshock tsunami which had yet to subside there.

2.6 Summary

In summary, large magnitude earthquakes do generate aftershocks that are potentially large enough to generate their own tsunami, particularly in the hours to days following the mainshock. However, it is often difficult to know if they did actually produce any tsunami themselves since the tsunami from the mainshock is typically continuing at the time. The Tohoku and New Ireland sequences are two good examples where aftershocks seem to have generated small to medium sized tsunami and the Sumatra 2004 is the best example where a probable aftershock (or triggered earthquake) has generated a large tsunami. Therefore, from these events and from commonly observed aftershock sequences from other, smaller, events, it seems reasonable to expect an increase in the potential tsunami hazard after a major subduction zone earthquake on the Hikurangi following the mainshock; either a from very large aftershock or from a triggered earthquake that occurs further along the zone. Note that the triggered earthquake may be larger than the mainshock. Although an earthquake with a magnitude above Mw 8.0 has not been observed to trigger an even larger event historically, there have not yet been very many earthquakes of this size so this possibility cannot be ruled out.

3.0 HYPOTHETICAL EARTHQUAKE CATALOGUE AND VIDEO

In order to provide an aftershock sequence inject for use in the exercise, we have taken the 2011 Tohoku earthquake sequence from the ISC-GEM catalogue and rotated and rescaled it to approximately fit the rupture zone of the exercise scenario's mainshock. We also reduced the magnitude of all events by 0.2 units since the Tohoku mainshock's magnitude was slightly larger than that for the scenario. The final map of earthquakes from just before the mainshock to about nine months afterwards is shown in Figure 3.1. The sequence fits the area covered by the rupture in the scenario well. Note that several of the remapped Mw 7.0 and greater earthquakes from the Tohoku sequence end up just underneath the Wairarapa after the transformation (green dots). They thus could be expected to cause significant shaking across the Greater Wellington Region. A simple animation of the first day of the aftershock sequence in its new location accompanies this report.

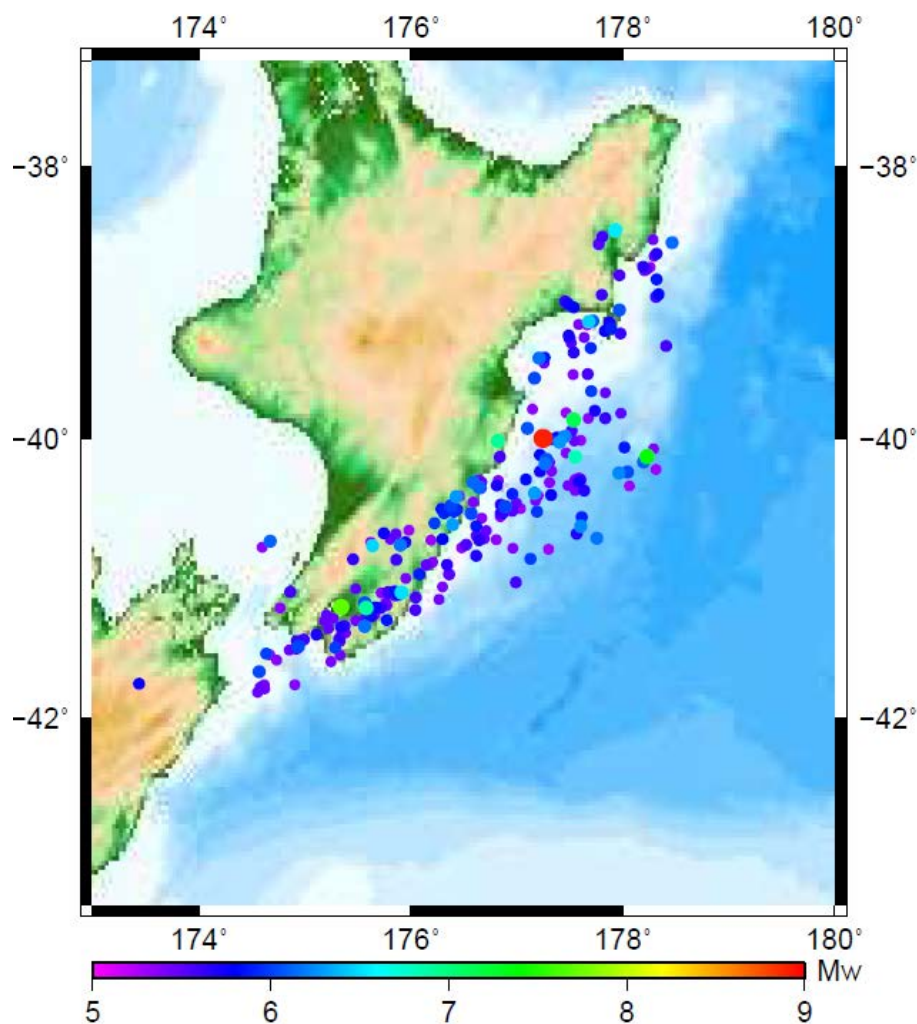


Figure 3.1 The proposed earthquake aftershock sequence for the scenario. It has been generated from the Tohoku aftershock sequence remapped and rescaled to fit the rupture zone of the scenario. The red dot is the location of the 2011 Tohoku earthquake's epicentre after the remapping. Only earthquakes above Mw 4.9 from 1 February 2011 (about one month before the earthquake) through to the end of 2011 are shown.

4.0 FORECAST PROBABILITY OF A MMI VI OR GREATER EARTHQUAKE

We map the probability of MMI VI or greater shaking occurring at least once during one-year periods starting one week and one year after an M8.9 subduction zone event, due to aftershocks triggered by the event. MMI VI is about the threshold when the shaking could be expected to begin to cause damage to buildings and other infrastructure depending on the details of that particular structure.

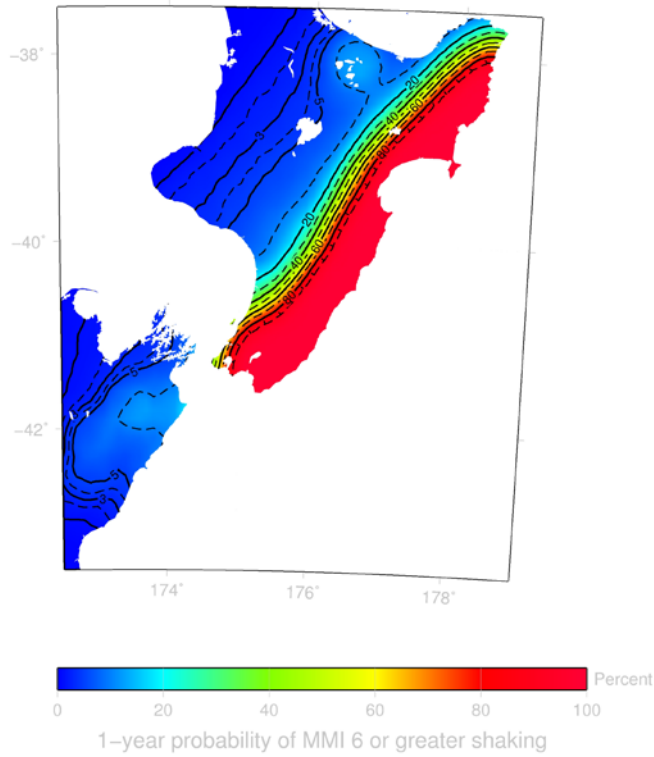
A map of expected number of aftershocks of Mw 5.0 and greater within spatial grid cells of 0.05 degrees during each target period was calculated using a space-time Epidemic-Type AfterShock (ETAS) model (Ogata 1998). The ETAS model regards every earthquake as a mainshock with its own aftershock sequence. The number of expected aftershocks of each event increases with the magnitude of the event, decays in time according to the Omori-Utsu relation (Utsu et al. 1995), and is distributed in space over an area that increases with the magnitude of the event. The model is applied to the whole earthquake catalogue prior to the start of the target forecasting period.

The version of the ETAS model used here is the one that has been tested in the New Zealand Earthquake Forecast Testing Centre over the past ten years (Gerstenberger and Rhoades 2010; Rhoades et al. 2018). To ensure the model works with the hypothetical catalogue we had adjusted the productivity parameter, κ , in the model since the hypothetical catalogue did not continue earthquakes below about 5.3. All other parameter values of the model were left at their standard values.

The map of expected aftershock occurrence was used to estimate the probability of earthquake shaking exceeding a given MMI. For this purpose, we generated 2000 synthetic earthquake catalogues over the one-year target period, with magnitudes between 5.0 and 8.5, based on the map of expected aftershock occurrence. For each earthquake in these catalogues, we simulated a value of MMI at every remote location using the Dowrick and Rhoades (2005) model for attenuation of MMI with distance from an earthquake source. The simulated MMI values take into account the estimated variability of MMI about the average. The probability of MMI exceeding a given level of MMI at each point in a dense grid was estimated as the proportion of the 2000 synthetic catalogues in which one or more earthquakes generates a simulated MMI value exceeding the given level.

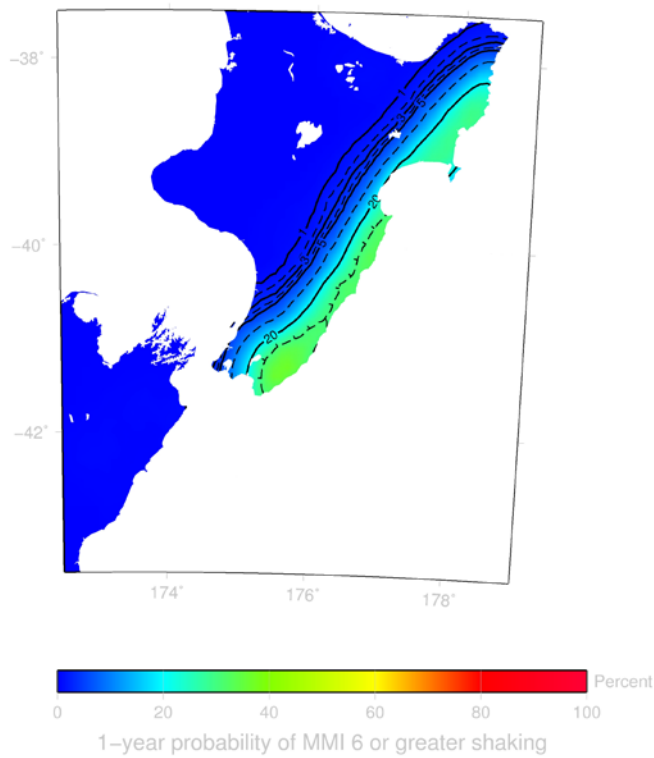
Figure 4.1a shows the probability of MMI VI or greater shaking over one year after a week has passed from the time of the mainshock. The probability that the east coast of the North Island will experience shaking of this intensity at least once over the next year is close to 100%. Once a year has passed, this probability drops to about 40% as the sequence subsides (Figure 4.1b). It should be noted that the MMI intensity maps estimate only the additional probability due to expected aftershocks of the earthquakes in the scenario catalogue. They do not include any long-term background contribution.

MMI 6



(a)

MMI 6



(b)

Figure 4.1 The probability that a point experiences shaking at above MMI VI from an aftershock generated by the M8.9 mainshock over the following 12 months. (a) shows this probability calculated one week after the mainshock and (b) shows the probability after one year has passed.

5.0 MMI FROM THE LARGEST AFTERSHOCK

To calculate the MMI from the largest aftershock we have used Shakemap. Shakemap was produced by the United States Geological Survey to provide near real-time estimates of ground motion and intensity following significant earthquakes. However, it can also be used to generate the intensity and ground motions expected from a hypothetical earthquake for a scenario as well. Note that Shakemap uses relatively simple equations to estimate intensity and ground motion in order to rapidly produce estimates of the median levels shaking that could be expected from an earthquake of a given magnitude. The modelling done in the previous proposal for the mainshock (using SPEC3D) uses fully three-dimensional equations to model seismic wave propagation for a specific earthquake, in that case the M8.9 mainshock.

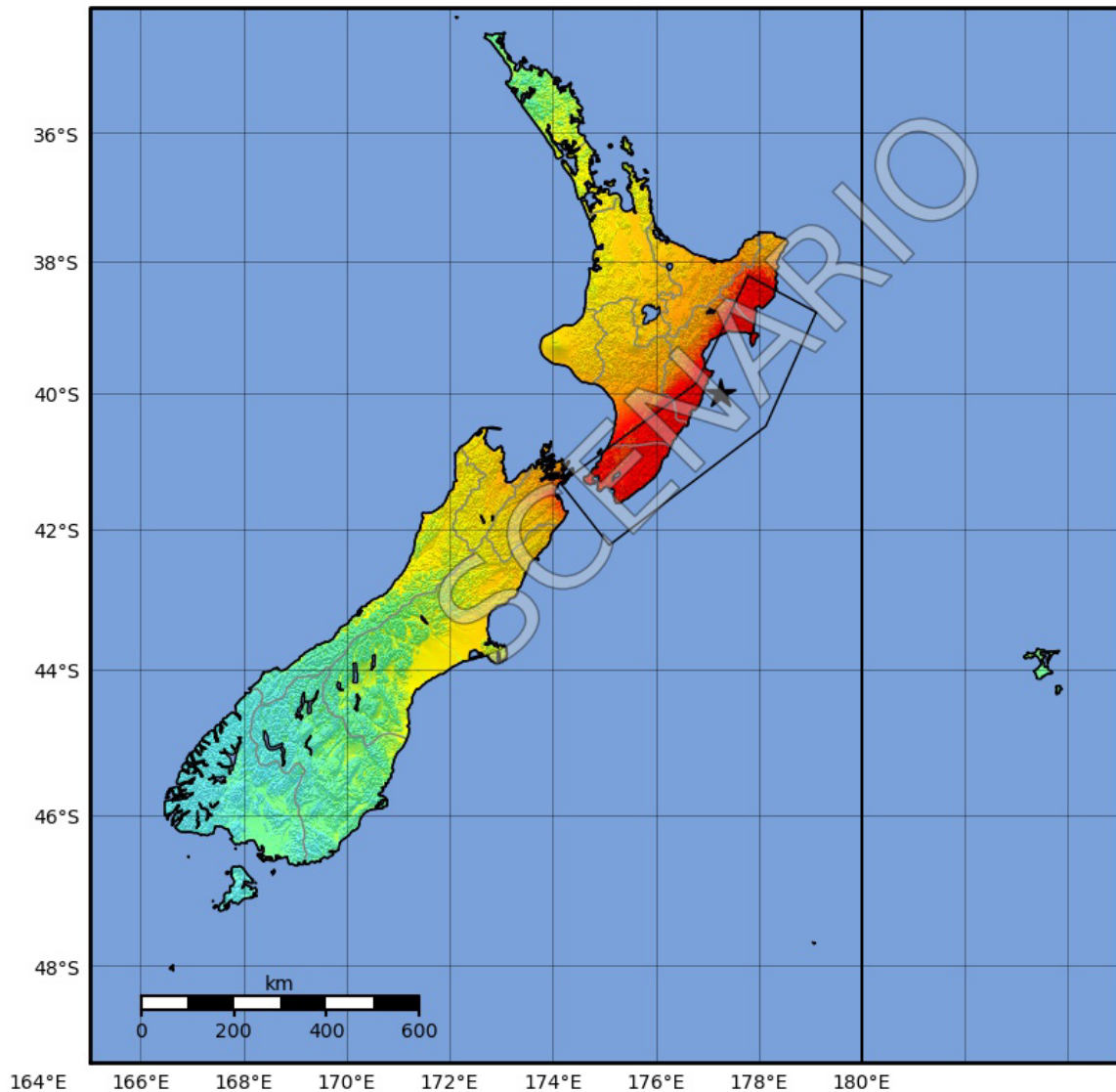
Shakemap has been used for that in many other exercises in New Zealand and elsewhere. For example, it was used to calculate the ground shaking for the scenario used in New Zealand's national tsunami exercise Tangaroa in 2016 (Burbidge et al. 2016).

To make sure the Shakemap intensities are comparable to the results from the previous SPEC3D modelling of the mainshock we have recalculated the ground motion intensities across New Zealand in Shakemap using an approximate representation of the earthquake rupture used in the scenario. The result is shown in Figure 5.1. Although the details are different, the general pattern is similar. The peak MMIs occur on the east coast of the North Island and go up to approximately MMI IX. Most of the North Island and the northern part of the South Island have MMIs greater than about VI and even the areas of New Zealand furthest from the rupture would experience MMIs between III and V. Note that this map should not be seen as a replacement for the original maps produced in the previous study since Shakemap estimates the median ground motion that could be expected at these locations, not the ground motion from that specific earthquake which can take into factors such rupture directivity.

The largest aftershock in the sequence is a rescaled magnitude Mw 7.7 earthquake that occurs near the southern end of the earthquake rupture about half an hour after the mainshock. To calculate the shaking using Shakemap we have used the rupture scaling relationship of Thingbaijam et al. (2017) to estimate an approximate length and width for this earthquake (about 120 km by 86 km). We then found the closest unit sources used in the original study to create an actual rupture length and width for this aftershock and aligned it to be approximately parallel to the plate margin. We then used Shakemap to estimate the ground motion intensities at both a national and regional scale (Figure 5.2). The outline of the aftershock's rupture area is shown by the black rectangle in Figure 5.2 and the epicentre by the black star. An earthquake of this size would generate substantial ground shaking in the Wairarapa (MMI VIII) and Wellington (MMI VII) and the surrounding region (MMVI). It would likely have been felt across much of New Zealand as well (Figure 5.2a). This amount of shaking from this event would be similar to that from 2016 Mw 7.8 earthquake in Ecuador (Chunga et al. 2018).

Note that these maps do not include the effect of sedimentary basins on ground motion. Basin effects amplified the shaking in areas such as downtown Wellington from the Kaikōura earthquake (Kaiser et al. 2017). This means that the shaking may be more intense than that shown in Figure 4.1 in areas where basin amplification is important.

Macroseismic Intensity Map
 GNS ShakeMap: Hikurangi, NZ
 Jul 09, 2019 15:31:00 UTC M8.9 S40.00 E177.25 Depth: 20.0km
 ID:gns00001_se



SHAKING	Not felt	Weak	Light	Moderate	Strong	Very strong	Severe	Violent	Extreme
DAMAGE	None	None	None	Very light	Light	Moderate	Moderate/heavy	Heavy	Very heavy
PGA(%g)	<0.05	0.3	2.76	6.2	11.5	21.5	40.1	74.7	>139
PGV(cm/s)	<0.02	0.13	1.41	4.65	9.64	20	41.4	85.8	>178
INTENSITY	I	II-III	IV	V	VI	VII	VIII	IX	X+

Scale based on Worden et al. (2012)

Version 1: Processed 2019-07-12T04:58:08Z

△ Seismic Instrument ○ Reported Intensity

★ Epicenter □ Rupture

Figure 5.1 Estimated MMI ground motion intensities for the mainshock rupture calculated using Shakemap. The black polygon shows the outline of the earthquake rupture projected onto the surface of the Earth.

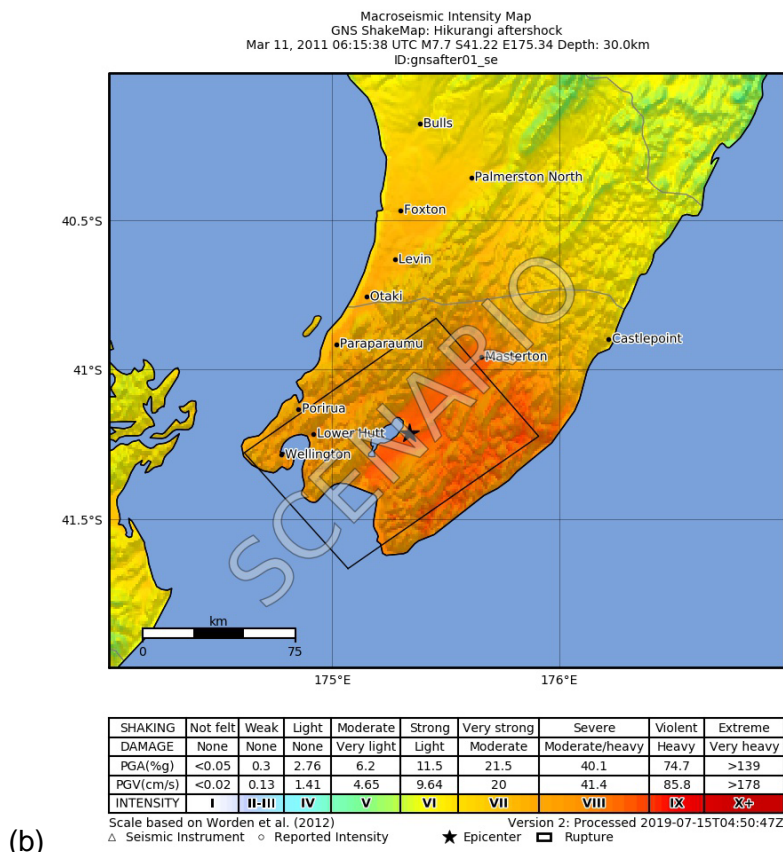
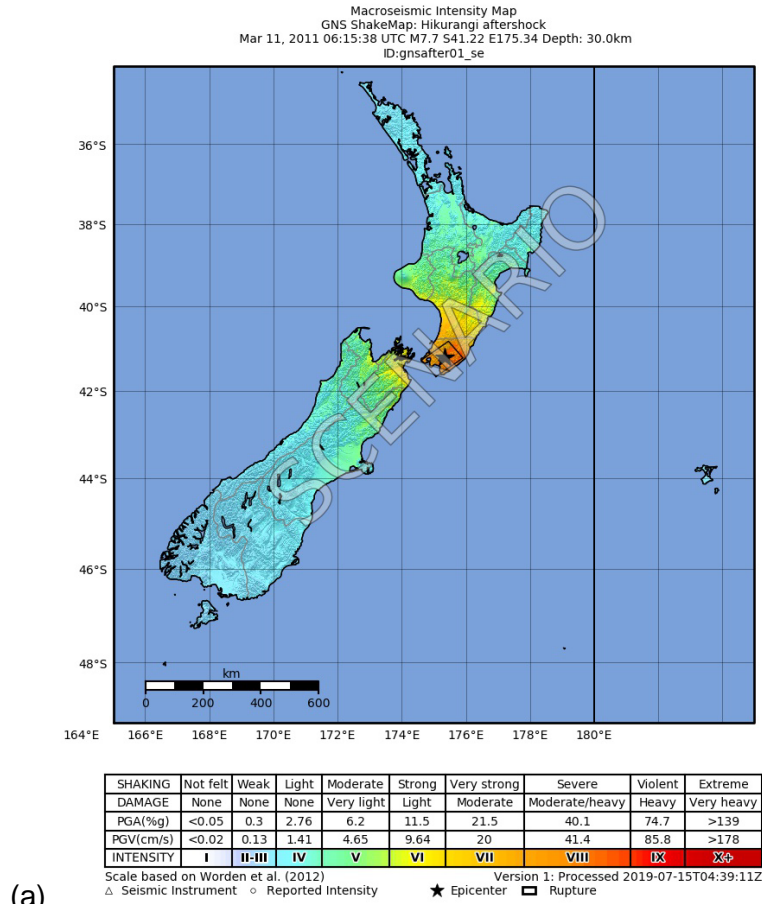


Figure 5.2 Estimated MMI ground motion intensities for the largest aftershock in the sequence calculated using Shakemap. (a) is drawn at a national scale and (b) is drawn at a regional scale. The black rectangle shows the outline of the aftershock rupture area used in the scenario.

6.0 PROBABILITY OF A TSUNAMIGENIC AFTERSHOCK

We assume a tsunamigenic aftershock to have at least a magnitude of 7.0 and therefore are interested in the probability of an aftershock of Mw 7.0 and larger to follow a Mw 8.9 mainshock. Note that we are excluding any tsunami generated by earthquake induced landslides from this calculation. Tsunamis generated by landslide may be generated by earthquakes smaller than Mw 7.0.

The decay of aftershock rate is most commonly described by the modified Omori law (Utsu et al. 1995). This is the oldest empirical relationship in seismology and goes back to the 1891 Nobi, Japan earthquake, where Omori (1894) described how the number of felt aftershocks per day decayed with time. Reasenber and Jones (1989) later showed how the Omori law could be related to the likelihood of an earthquake of a given magnitude given by the Gutenberg and Richter (1944) relationship. To calculate the expected daily, monthly (30 days) and yearly (365 days) rate of aftershocks of M7+ rate here we use the generic parameters for the Reasenber-Jones formation of the Omori Law for subduction zones described in Page et al. (2016). Given that some of the aftershocks will occur on land, we reduce the resulting rate by one third. To then derive the probability, we assume the aftershocks follow a Poisson distribution where the likelihood of an aftershock is independent of the time since the last event. Figure 6.1 shows how the resulting daily, monthly and yearly probabilities as they decay over time. According to the figure, the chance for an offshore earthquake above Mw 7 over the next year starts just below 100% but decays to about 50% after a year.

We note that Page et al. (2016) observed that the aftershock rate between sequences within the same tectonic region can vary by a factor of 10 and more. Therefore, this can give a large amount of variability in these probabilities. The calculated probabilities in Figure 6.1 therefore only reflect those for an average sequence. For example, a variation of the rate by a factor of 10 would mean that the daily probability on day 1 could vary between 9% and 62% (average 26%). A change in rate of 10 for the annual probability would vary the probability between 69% and 100% on day 1 with the average being 98%. Figure 6.1 thus only provides shows how the probabilities decay with time on average after a major subduction event.

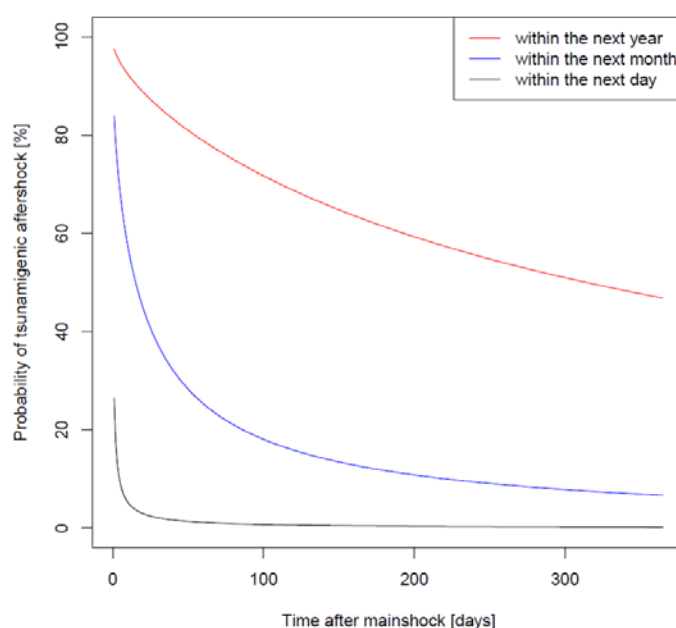


Figure 6.1 The average probability (%) of one or more Mw 7 or larger to follow a mainshock of magnitude 8.9 within the next year (red), month (blue) and day (black) for a year after the mainshock.

7.0 QUALITATIVE AFTERSHOCK IMPACT ASSESSMENT

The following aftershock impact scenario was developed by an 'expert panel' meeting between William Power, Julia Becker, ShengLin Lin and David Burbidge. It was informed by the other injects developed described above and the previous impacts from the mainshock described in Power et al. (2018).

As with the previous impact assessment by Power et al. (2018), the development of the scenario was entirely qualitative and based solely on the judgment of the expert panel. No additional research or literature review was undertaken. It must be assumed that quantitative loss analysis, or qualitative loss analysis by experts in more specific fields (e.g. landslides or fire risk) will yield significant changes to this scenario.

Where specific impact locations, or numbers of affected properties or people, are presented in this scenario, the choice is essentially arbitrary within the plausible range of possibilities as judged by the panel. For example, we expect additional landslides to be one of the issues to be faced after a large aftershock, but the specific choice of Kelson in Wellington as the location is arbitrary.

This approach to developing the scenario, whereby apparently specific details are provided without specific motivations for the choices made, has been used for the purpose of developing the impacts from the aftershocks for the exercise. It is the same approach as was used by Power et al. (2018) for the mainshock used in the exercise. In particular, we stress that the choices of particular locations or quantities must **not** be used as the basis for assessing the risk to any particular property or person and must **not** be used as the basis for any site-specific engineering work.

7.1 Big Picture

The mainshock of the exercise was assumed to occur just after 9am on a winter school day. About half an hour after the mainshock at about 9:30 am a Mw 7.7 aftershock occurs on the subduction zone underneath the Wellington Region. An earthquake of this size can be expected to be about 120 x 80 km in area and dip to the northwest. This would mean that the deepest part of the rupture would be below Wellington and it will become steadily shallower to the southeast. The shaking is shown in Figure 5.2 and ranges from MMI VIII to VII across the Wellington region and MMI VII to VI in Marlborough and Manawatu regions. Further to the north or south in New Zealand the intensity decreases reaching a minimum of about MMI III in Southland. In any given region the actual felt intensity will be higher or lower than the region's typical value depending on the details of the local soil conditions. For example, shaking will typically be more intense in the Hutt Valley than in the surrounding hills.

7.2 Wellington, Porirua and Hutt Valley

Given this distribution of shaking most of the impacts from this particular aftershock are in the Wellington region.

In the mainshock 50 buildings in Wellington collapsed partially or catastrophically and about 25% of buildings were damaged beyond the possibility of repair. In this aftershock an additional 25 buildings collapse partially or catastrophically. These buildings are all ones that were severely damaged in the earlier mainshock. Another 8.5% of the buildings in Wellington are damaged beyond repair. The total number of collapsed buildings from the mainshock and this

aftershock combined is 75 and a total of 33.5% of buildings in Wellington are now damaged beyond repair.

The aftershock triggers further landslides across the region. A new landslide occurs in the upper reaches of the Hutt Valley in the Kaitoke Gorge blocking the Hutt river. Another landslide occurs in Kelson engulfing 10 houses and a further landslide occurs in Stokes Valley engulfing 5 houses. Landslides from the mainshock have already isolated Wellington. The aftershock causes further smaller landslides at other points of SH1 and SH2 making access to Wellington even more difficult and increasing the time to clear the highway.

The tsunami from the mainshock arrives in the inner harbour at about the same time as the aftershock occurs. The aftershock itself is mostly onshore so does not add significantly to this tsunami. Inundation extents and run-up heights would be broadly the same as those estimated from the mainshock's tsunami in Power et al. (2018).

Seventy-five percent of the population in the Wellington CBD has evacuated the tsunami inundation zones by the time of the aftershock, the rest remain within office buildings. Outside of the CBD about 85% of the population within the tsunami evacuation zones have decided to evacuate. Those that stayed are disproportionately elderly or disabled, others have stayed because they were unaware that they were in an evacuation zone or have chosen to stay to help family members unable to leave. Seventy-five percent have succeeded in leaving the evacuation zone and 10% are still in the process of leaving when the aftershock occurs. Those still leaving are disproportionately slower walkers or the disabled. Most of those evacuating at this point are on foot, as those who left by car have either succeeded or have abandoned their vehicles. Those that are still evacuating (or have evacuated but not found suitable shelter or open ground) are now outside and vulnerable to injury from falling debris from nearby buildings. The shaking is sufficiently intense that the evacuation halts until the shaking subsides enough to continue evacuating. This will take a minute or so.

In areas outside of the tsunami evacuation zones, much of the population have remained where they were during the mainshock and have not evacuated the buildings they were in at 9am. However, five of these buildings then collapse in the aftershock, resulting in further deaths and injuries. Those that have left their buildings would be exposed to falling debris and some are injured and killed by this debris.

The mainshock caused an oil spill in Seaview and minor fires. More oil is spilled from the shaking caused by the aftershock and the minor fires now combine to become a major fire.

Areas that liquefied in the mainshock will experience further liquefaction due to the aftershock, increasing the level of damage in those areas.

Utilities, with the exception of telecommunications, were already all cut off by the mainshock. The aftershock will further damage them and result in longer repair times. Telecommunications will continue for a further eight hours under battery power and is not significantly worsened by the aftershock. However, communication by mobile phone is likely to be difficult or impossible in the initial period following the mainshock.

In total a further 50 people are killed by the aftershock and another 1000 are injured in Wellington, Kapiti Coast and the Hutt Valley by the aftershock. This is in addition to the numbers killed or injured by the mainshock and its secondary impacts (fires, landslides and tsunami) described in the previous assessment.

7.3 Greater Wellington Region

Wairarapa experiences some of the largest levels of shaking from this aftershock (MMI VIII). Buildings damaged by the mainshock are further damaged and about 10 collapse. An additional 25 people are killed in the Greater Wellington Region outside of Wellington City and the Hutt Valley/Porirua areas, mostly in the Wairarapa, and a further 1000 are injured. More landslides occur across the region making access to remote areas even more difficult.

7.4 Outside Greater Wellington Region

Outside the Greater Wellington region the shaking will mostly just be interpreted as just another aftershock; one of many aftershocks they are currently experiencing. The shaking is likely to be strong enough to slow down the evacuation in the Hawkes Bay region. However, this is likely to also be the case for the other aftershocks which are smaller in magnitude but closer. Given that the shaking is still fairly high, another 50 people are injured across wider New Zealand from falling debris or objects, mostly in Manawatu, Marlborough and Hawkes Bay. Some more buildings in those areas also experience minor damage. However, no other buildings outside the Greater Wellington Region collapse from this aftershock. No additional fatalities occur outside the Greater Wellington Region.

7.5 Aftershock Sequence

The above scenario describes the impact from this particular aftershock. This is the largest aftershock in this hypothetical sequence but one of many that are occurring across the region. Aftershocks are the most frequent on the first day after the mainshock but continue semi-continuously for the first few weeks (see Figure 4.1 and Figure 6.1). Aftershocks continue more sporadically over the months and years to come. Many of the more intense aftershocks will lead to injuries or further damage weakened buildings. All events close enough to the coast to cause MMI VI shaking or greater lead to further self-evacuation from the coastal parts of New Zealand. Emergency service personnel in those areas will likely have to repeatedly evacuate from the area every time there is a large aftershock nearby, slowing rescue efforts in the first few days. Repair efforts in other parts of the New Zealand are also likely to be slowed by the semi-continuous series of aftershocks in the first few weeks.

The general public will probably not wish to return to the areas impacted by the tsunami for the first few weeks at least. The semi-continuous sequence of aftershocks over such a long period of time will have severe psycho-social impacts across the population in the affected area. The population will become increasingly exhausted, anxious and highly stressed. Many will also have lost their homes and family members. Others will have become separated from family members for an extended period of time after the mainshock.

Workplaces across the east coast of the North Island will mostly shut down for at least the first few weeks after the event leading to further downstream impacts. The mainshock and its aftershock sequence will have a long lasting economic impact on New Zealand that will be felt for years to come, particularly in areas such as tourism.

8.0 ACKNOWLEDGEMENTS

The authors would like to thank Finn Scheele and Yoshihiro Kaneko for reviewing the report.

9.0 REFERENCES

- Burbidge DR, Power WL, Horspool NA. 2016. The tsunami scenario for the Exercise Tangaroa 2016. Lower Hutt (NZ): GNS Science. 16 p. Consultancy Report 2016/20. Prepared for: Ministry of Civil Defence & Emergency Management (MCDEM).
- Christophersen A, Smith EGC. 2008. Foreshock rates from aftershock abundance. *Bulletin of the Seismological Society of America*. 98(5):2133–2148. doi:10.1785/0120060143.
- Chunga K, Livio F, Mulas M, Ochoa-Cornejo F, Besenon D, Ferrario MF, Michetti AM. 2018. Earthquake ground effects and intensity of the 16 April 2016 Mw 7.8 Pedernales, Ecuador, earthquake: implications for the source characterization of large subduction earthquakes. *Bulletin of the Seismological Society of America*. 108(6):3384–3397. doi:10.1785/0120180051.
- Dowrick DJ, Rhoades DA. 2005. Revised models for attenuation of Modified Mercalli intensity in New Zealand earthquakes. *Bulletin of the New Zealand Society for Earthquake Engineering*. 38(4):185–214.
- Gahalaut VK, Gahalaut K. 2005. 29 March 2005 Sumatra earthquake: expected, triggered or aftershock? *Current Science*. 89(3):452–454.
- Geist EL, Parsons T. 2005. Triggering of tsunamigenic aftershocks from large strike-slip earthquakes: analysis of the November 2000 New Ireland earthquake sequence. *Geochemistry, Geophysics, Geosystems*. 6(10):Q10005. doi:10.1029/2005gc000935.
- Gerstenberger MC, Rhoades DA. 2010. New Zealand Earthquake Forecast Testing Centre. *Pure and Applied Geophysics*. 167(8–9) 877–892; doi:10.1007/s00024-010-0082-4.
- Gutenberg R, Richter CF. 1944. Frequency of earthquakes in California. *Bulletin of the Seismological Society of America*. 34(4):185–188.
- Kaiser AE, Balfour NJ, Fry B, Holden C, Litchfield NJ, Gerstenberger MC, D'Anastasio E, Horspool NA, McVerry GH, Ristau J, et al. 2017. The 2016 Kaikoura, New Zealand, earthquake: preliminary seismological report. *Seismological Research Letters*. 88(3):727–739. doi:10.1785/0220170018.
- International Seismological Centre, ISC-GEM Earthquake Catalogue. Berkshire (GB): International Seismological Centre; [accessed 2019 Jul 2]. <https://doi.org/10.31905/d808b825>.
- National Geophysical Data Centre/World Data Service: NCEI/WDS Global Historical Tsunami Database. Boulder (CO): NOAA National Centers for Environmental Information; [accessed 2019 Jul 8]. doi:10.7289/V5PN93H7. https://www.ngdc.noaa.gov/hazard/tsu_db.shtml.
- Ogata Y. 1998. Space-time point-process models for earthquake occurrences. *Annals of the Institute of Statistical Mathematics*. 50(2):379–402. doi:10.1023/A:1003403601725.
- Omori F. 1894. On aftershocks. Report of Imperial Earthquake Investigation Committee. 2:103–109.
- Page MT, van der Elst N, Hardebeck J, Felzer K, Michael AJ. 2016. Three ingredients for improved global aftershock forecasts: tectonic region, time-dependent catalog incompleteness, and intersequence variability. *Bulletin of the Seismological Society of America*. 106(5):2290–2301.

- Power WL, Kaneko Y, Becker JS, Lin S-L, Holden C, Mueller C. 2018. Hikurangi response plan: developing a scenario for an Mw 8.9 Hikurangi earthquake, including tsunami modelling and a preliminary description of impacts. Lower Hutt (NZ): GNS Science. 39 p. Consultancy Report 2018/168. Prepared for Hawke's Bay Regional Council.
- Reasenber PA, Jones LM. 1989. Earthquake hazard after a mainshock in California. *Science*. 243(4895):1173–1176.
- Rhoades DA, Christophersen A, Gerstenberger MC, Liukis M, Silva F, Marzocchi W, Werner MJ, Jordan TH. 2018. Highlights from the first ten years of the New Zealand Earthquake Forecast Center. *Seismological Research Letters*. 89(4):1229–1237. doi:10.1785/0220180032.
- Scholz CH. 2002. *The mechanics of earthquakes and faulting*. 2nd ed. Cambridge (GB): Cambridge University Press. 471 p.
- Thingbaijam KKS, Martin Mai P, Goda K. 2017. New empirical earthquake source-scaling laws. *Bulletin of the Seismological Society of America*. 107(5):2225–2246. doi:10.1785/0120170017.
- Utsu T, Ogata Y, S R, Matsu'ura. 1995. The centenary of the Omori formula for a decay law of aftershock activity. *Journal of Physics of the Earth*. 43(1):1–33. doi:10.4294/jpe1952.43.1.
- Worden CB, Gerstenberger MC, Rhoades DA, Wald DJ. 2012. Probabilistic relationships between ground-motion parameters and Modified Mercalli intensity in California. *Bulletin of the Seismological Society of America*. 102(1):204–221. doi:10.1785/0120110156.



www.gns.cri.nz

Principal Location

1 Fairway Drive
Avalon
PO Box 30368
Lower Hutt
New Zealand
T +64-4-570 1444
F +64-4-570 4600

Other Locations

Dunedin Research Centre
764 Cumberland Street
Private Bag 1930
Dunedin
New Zealand
T +64-3-477 4050
F +64-3-477 5232

Wairakei Research Centre
114 Karetoto Road
Wairakei
Private Bag 2000, Taupo
New Zealand
T +64-7-374 8211
F +64-7-374 8199

National Isotope Centre
30 Gracefield Road
PO Box 31312
Lower Hutt
New Zealand
T +64-4-570 1444
F +64-4-570 4657